Anomalous properties of a large magnetic moment in a fourfold potential

2003 J. Phys.: Condens. Matter 15 3417

(http://iopscience.iop.org/0953-8984/15/20/305)

INSTITUTE OF PHYSICS PUBLISHING JOURNAL OF PHYSICS: CONDENSED MATTER

J. Phys.: Condens. Matter **15** (2003) 3417–3432 PII: S0953-8984(03)58499-5

Anomalous properties of a large magnetic moment in a fourfold potential

Nicolas Vernier and Guy Bellessa

Laboratoire de Physique des Solides, Bâtiment 510, Université Paris-Sud, F-91405 Orsay, France

Received 20 January 2003
Published 12 May 2003
Online at stacks.iop.org/JPhysCM/15/3417

Abstract

An experimental study of magnetic moments placed in a fourfold potential is presented here. The system used is a monocrystal of $LiY_{0.99}Dy_{0.01}F_4$, where the only magnetic ions are the Dy^{3+} ions. From static magnetic susceptibility measurements, it is shown that the Dy^{3+} ion has an easy magnetization plane, with an additional anisotropy in the easy plane. Low frequency electron paramagnetic resonance experiments are presented here and up to nine resonance lines have been found. Some of them are in agreement with known properties of the Dy^{3+} ion in $LiY_{0.99}Dy_{0.01}F_4$, but others cannot be explained within the framework of the commonly used effective Hamiltonian. The behaviour of these new lines is consistent with a magnetic tunnelling effect. Finally, spin echoes have been observed, allowing the determination of the relaxation time T_2 and the coupling coefficient for several orientations of the magnetic field.

1. Introduction

As technology keeps on progressing, it has become possible to make systems smaller and smaller. These systems are approaching the limits for which quantum effects are expected to become very important. It is especially true for magnetic nanoparticles: reversal of the magnetization of small particles because of a tunnelling effect has become the subject of intense investigation. This phenomenon has been studied now for about 20 years. First, the case of a large magnetic moment (which means a magnetic moment with a large value of the quantum number J) which has an easy anisotropy axis has been treated: it has been shown theoretically [1–5] that an orthogonal static magnetic field could couple the fundamental doublet $J_z = \pm J$, allowing the reversal of J_z. A lot of work has been done using this configuration, the anisotropy being described by the term $-DJ_z^2$ in the Hamiltonian. It has been shown that the process could be stimulated by several processes: phonon interactions [6], hyperfine interactions [7] and non-axial anisotropy such as the one described by the terms J_x^2 [8] or $(J_x^4 + J_y^4)$ [9]. From the experimental point of view, the first evidence of this tunnelling effect was found with glasses doped with rare-earth ions [10]. Recently, clusters of $AcMn_{12}$

and Fe_8 have been synthesized: it has quickly emerged that they are a good model system for this purpose and, indeed, strong evidence for a tunnelling reversal have been found [11–15]. Recently, other types of anisotropies have come into focus: the case of an easy plane with two easy directions in the plane [16] and the cubic symmetry, for which three or four easy directions are expected [17].

Here, a set of results obtained with a model system which may belong to one of these new cases is reported (preliminary results have already been published [18]: a complete analysis is presented here): a monocrystal doped with magnetic rare-earth ions. A crystal with an easy magnetization plane has been chosen. Because of the electrostatic crystal field, some easier directions are expected in the plane, which agrees with static magnetic susceptibility measurements presented here. To get only the fundamental states, the sample was cooled down to very low temperature (the anisotropy in the easy plane is due to high order terms). As the main idea behind this work was the possible occurrence of tunnelling and as the splitting arising from this effect is often very small, we have chosen to work at low frequency. EPR results at 10 GHz being already available from previous studies and tunnelling being often highly non-linear, it was interesting to try another frequency below 10 GHz. This approach was successful: it has been possible to find new behaviours consistent with tunnelling theory.

2. Experimental set-up

2.1. Sample

The sample belongs to the $LiRF_4$ category. The unit cell is tetragonal and body-centred [19] and its symmetry space group is almost D_{2d}. The composition of the sample was $LiY_{0.99}Dy_{0.01}F_4$. It is insulating, transparent and colourless. The only magnetic ion in this compound is Dy^{3+}, which takes the place of Y^{3+} on the R sites. Dy^{3+} is a Kramers ion (J is half-integer), with a quite large quantum number $J = 15/2$. Because of the high dilution of these magnetic ions, the mean distance between two ions is quite large (about 10 atomic distances). So, to first order, interactions between ions can be neglected and it can be considered that every ion has the same environment. The sample was a single crystal. It has been oriented with the Laue procedure, then it has been cut as a parallelepiped of size $4 \times 4 \times 5$ mm^3. The faces have been chosen to be parallel to the [110], [1$\bar{1}$0] and [001] directions.

From a preceding EPR study by other authors, the following values have been found for the phenomenological parameters $g_\parallel$ and $g_\perp$ ($g_\parallel$ is the effective Landé factor when the static magnetic field is parallel to the direction [001]): $g_\parallel = 1.11$ and $g_\perp = 9.2$ [20, 21]. It means that, in $LiRF_4$, there is an easy plane for the magnetic moment of the Dy^{3+} ion. The easy plane is orthogonal to the [001] direction. The magnetization of the sample as a function of the magnetic field was measured with a SQUID magnetometer, to check the anisotropy. The magnetization was obtained with an extraction procedure, which gave the component of the magnetization parallel to the static magnetic field. The magnetic field was swept in the range from zero to 5 T. The measurements were performed at the lowest temperature possible, which was 2 K.

2.2. Electron paramagnetic resonance apparatus

The EPR apparatus is a very low frequency one: the sample is put in the centre of a split-ring resonator, also called a loop-gap resonator [22]. The frequency of resonance is around 680 MHz and the quality factor is around 3000 at low temperature. The characteristics of the resonator do not change in the range of temperature [10 mK, 10 K]. This was checked

by doing a test with nothing in the resonator. This kind of resonator was chosen because, in the centre of the resonator, the oscillating electric field is almost zero; there is only an oscillating magnetic field. So there is no mixing with some dielectric effect. The amplitude of the magnetic oscillating B_1 could be chosen between 10^{-8} and 10^{-3} T. A static magnetic field B_0 up to 5 T, perpendicular to B_1, could be applied with a superconducting coil. The magnetic susceptibility χ' and χ'' of the sample was obtained from the frequency response of the resonator: the shape of the signal as a function of the frequency is Lorentzian. If f_0 and Δf_0 are the resonance frequency and the linewidth of the empty resonator, respectively, and f and Δf are the resonance frequency and the linewidth of the resonator with the sample, respectively, then, at first order, χ' and χ'' are given by the following formulae [23]:

$$\begin{aligned} \chi' &= \frac{2}{\alpha}\frac{f - f_0}{f_0} \\ \chi'' &= \frac{1}{\alpha}\frac{\Delta f - \Delta f_0}{f_0} \end{aligned} \tag{1}$$

where α is the filling factor of the resonator. In the case of the present sample, $\alpha = 0.09$.

2.3. Low temperature

For this study, it is important to work at very low temperature, otherwise thermal activation might dominate the tunnelling process. The very low temperatures are obtained with a He^3–He^4 dilution refrigerator, which could reach 17 mK. The whole resonator was screwed to the cool end of the refrigerator. The sample was stuck at the end of a glass parallelepiped, which was itself thermalized on the cool end of the refrigerator. The thermal conductivity of the glass was large enough to get a good thermalization of the sample, even at the lowest temperature. Experimentally, thermalization was checked by lowering the power: there was no more variation of χ' and χ'' in the range of very low powers. The temperature was measured with a Matsushita carbon resistance thermometer [24]. This kind of resistance thermometer has a very low magnetoresistance and can be used even in high magnetic fields.

When working at very low temperature, it is necessary to use a power as small as possible, otherwise the refrigerator will not reach the lowest temperature. Therefore, to reduce the input power needed for the measurements, the high frequency excitation was applied in short pulses. To get χ' and χ'', the pulses had to be long enough in order to reach the steady state of the resonator. This was realized after 2 or 3 μs, and 13 μs was chosen for the duration of the pulses. The pulses were sent with a rate ranging from 100 to 0.001 Hz, depending on the instantaneous power. It was also possible to reduce the duration of the pulses, and to send sequences of several pulses. Thus, it was possible to perform spin echo experiments [25]. To analyse the signal in the cavity, only the envelope of the pulse is kept with the use of a phase-sensitive device. In order to have the amplitude of the signal, the dephasing between the reference and the signal in the mixing stage could be varied continuously. The envelope of the signal could be visualized with an oscilloscope or digitized and transferred to computer for a numerical treatment.

3. Static magnetic susceptibility

The magnetization was measured for three orientations of the sample at a temperature of 2 K: first, the static field was parallel to the [001] axis (i.e. orthogonal to the easy plane). Then, the [100] and [110] directions in the easy plane were studied (because of symmetry, the [010] direction should be similar to the [100] direction). The parallel magnetization as a function of

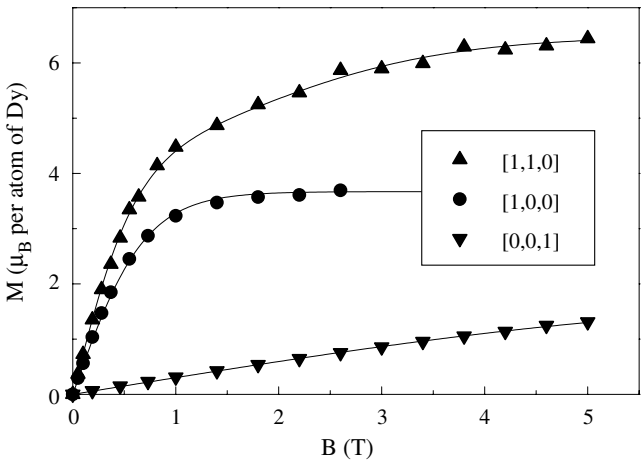

Figure 1. Static magnetization per atom of dysprosium as a function of the magnetic field B, for different orientations of the sample, at the temperature of $T = 2$ K. The measured component of the magnetization is the one parallel to the applied magnetic field. The straight lines are guides for the eye.

the magnetic field in these three cases is shown in figure 1. When the magnetic field is applied in the [001] direction, the magnetization increases slowly and almost linearly. Even at 5 T, the magnetization is far from saturation: there is only 1.5 μ_B/atom of dysprosium. When the magnetic field is applied in the [110] direction, the magnetization increases very quickly until 1 T, and above this value, the magnetization seems to go more and more slowly to saturation. At 5 T, the saturation is not reached yet, but it is not very far away. When the magnetic field is applied in the [100] direction, the behaviour is quite different: the magnetization increases very quickly until 1 T, and above this value, the magnetization saturates at around 4 μ_B, which is only about half of the expected value for the saturation magnetization.

From the preceding results, the first conclusion is that, as expected, there is an easy plane for the magnetization, which is perpendicular to the [001] axis. Next, it appears that all the directions are not similar in the easy plane, as shown by the two different behaviours obtained for the two directions in the easy plane. Several of these features can be explained using the quite simple model of [16]. The authors have introduced an anisotropy in the easy plane with a term of the type $(J_x^4 + J_y^4)$ and they have shown that, in low magnetic field, the resulting susceptibility is not isotropic in the easy plane. To go further, one has to know what happens at high magnetic field.

Using the model developed in [16], the magnetization over the whole range of magnetic field has been evaluated. One more hypothesis has been assumed: the gap between the ground doublet and the first excited doublet remains much larger than the Zeeman splitting in the whole range of magnetic field. It gives a saturation magnetization depending on the direction of the magnetic field, which agrees with the experiment. It has been possible to obtain a very good fit in the case where the magnetic field is parallel to the [100] axis, and the saturation magnetization agreed quite well with the expected value, which is $J/2$. When the magnetic field is parallel to one of the easy axes, the saturation magnetization should be $J/\sqrt{2}$. Experimentally, the saturation magnetization is indeed larger. So far, so good, and there is qualitative agreement between what is expected from theory and what is observed experimentally. However, when the last case is analysed closer, some discrepancies appear between theory and experiment. Firstly, the magnetization should be saturated above

1.5 T, but even at 5 T, saturation is not yet reached. Secondly, the ratio of the two saturation magnetizations (for the directions [110] and [100]) should be $\sqrt{2}$, but experimentally it is larger than 1.8. So it seems that the model needs to be slightly improved.

4. EPR spectra

Up to now, for a given orientation of the sample, measurements made with an X-band EPR spectrometer had revealed only one line [20, 21]. Here, using a very low frequency spectrometer, many new lines have been found. The different lines have been numbered to help reference them. Several of these lines have a very unusual shape.

4.1. Low field lines

Lines 1, 2 and 2′ have been obtained for the external applied field parallel to [001], [110] and [1$\bar{1}$0] respectively. Lines 1 and 2 have been plotted in figure 2 (line 2′ is similar to line 2 and has not been plotted). Their shapes are quite unusual: they are quite strongly asymmetrical. It is especially obvious with χ' in figure 2(b), where there is no negative hump on the low field side (i.e. B is lower than B_R), as would have been expected from the well-known formula (2) following [26]:

$$\begin{aligned} M' &= \frac{\beta(B - B_R)T_2^2}{1 + \gamma^2 T_2^2 (B_R - B)^2} M_0 \\ M'' &= \frac{\beta T_2}{1 + \gamma^2 T_2^2 (B_R - B)^2} M_0 \end{aligned} \tag{2}$$

where B_R is the magnetic field for which the resonance occurs, T_2 is the transverse relaxation time and β is the coupling coefficient. B is the total magnetic field acting on the spin and M_0 is the thermal equilibrium value of the resonating spin in the magnetic field B.

The distorted shape of the low field lines can be explained by the unusually low frequency used in the present work. Indeed, for low field resonance, the lineshapes are very sensitive to two effects, which are the inhomogenous broadening and the existence of two rotary polarizations (the experimental device provides a linear polarization, which is the superposition of two rotary polarizations). As these effects are most often negligible, they are almost always ignored. Therefore, a quick summary of the calculation is presented here.

B is the sum of the external applied magnetic field and the local internal field. A Lorentzian has been assumed for the distribution of the local magnetic field. M_0 can be calculated using a Boltzmann statistic, assuming the temperature to be much higher than the Zeeman energy. M_0 becomes a linear function of B. Then, M' and M'' can be obtained by summing the magnetization over the distribution of the local magnetic field. Although quite long, the integration can be done using standard methods [27]. Adding the contribution of the two rotary components, χ' and χ'' can be deduced and are given by the following formulae:

$$\begin{aligned} \chi' &= \mu_0 N \frac{\gamma_1^2 \hbar^2}{8 k_B T} \left[\frac{B_0^2 + B_0 \cdot B_R + \Delta B^2}{\Delta B^2 + (B_0 + B_R)^2} + \frac{B_0^2 - B_0 \cdot B_R + \Delta B^2}{\Delta B^2 + (B_0 - B_R)^2} \right] \\ \chi'' &= \mu_0 N \frac{\gamma_1^2 \hbar^2}{8 k_B T} \left[\frac{B_R \cdot \Delta B}{\Delta B^2 + (B_0 + B_R)^2} + \frac{B_R \cdot \Delta B}{\Delta B^2 + (B_0 - B_R)^2} \right] \end{aligned} \tag{3}$$

where N is the density of spins, $\gamma_1 = 2\beta/\hbar B_1$, B_1 is the oscillating magnetic field (the μ_0 prefactor comes from the approximation $H_1 = B_1/\mu_0$, which is justified when $\chi \ll 1$) and B_0 is the external applied magnetic field. For high B_R value lines, M_0 may no longer be a linear

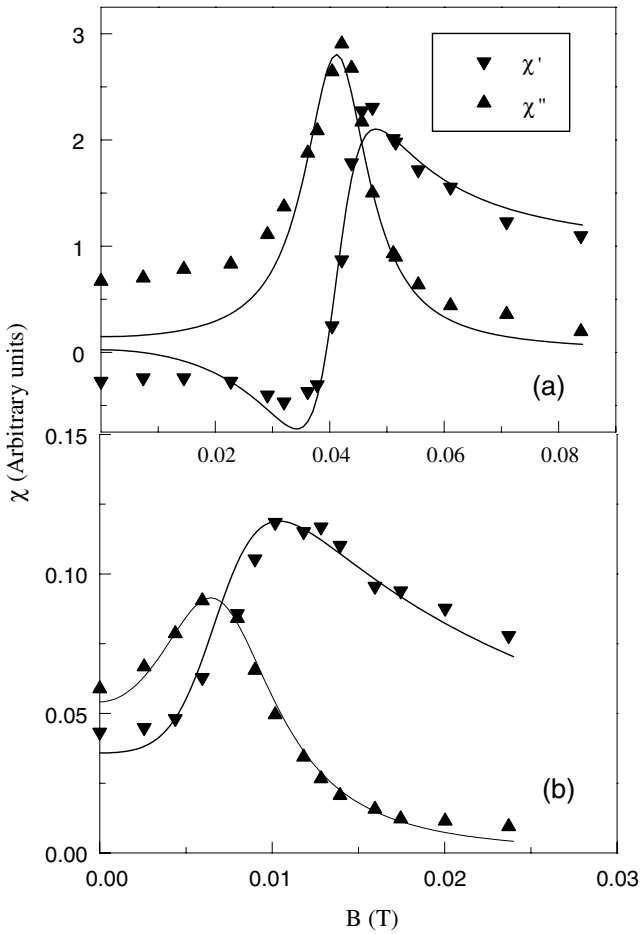

Figure 2. (a) Real and imaginary part of the susceptibility for line 1 at temperature $T = 4.2$ K. The static field B_0 is parallel to [001] and the oscillating field B_1 is parallel to [110]. (b) Real and imaginary part of the susceptibility for line 2 at temperature $T = 43$ mK. The static field B_0 is parallel to [110] and the oscillating field B_1 is parallel to $[1\bar{1}0]$.

function of B. However, this mistake can be corrected afterwards within a good approximation by multiplying the final result (3) by the factor $\alpha(B_0)$:

$$\alpha(B_0) = \frac{\tanh(g_{eff}\mu_B B_0/2kT)}{g_{eff}\mu_B B_0/2kT}. \tag{4}$$

Using the above formulae (3) and (4), it has been possible to get a good agreement with the experimental results, as can be seen in figure 2, where the full curves hold for the best fits obtained.

4.2. High field lines

For B_0 parallel to [110] and B_1 parallel to $[1\bar{1}0]$, at least four lines have been found. They are plotted in figure 3.

Between 50 and 250 mT, see figure 3(a), there is a broad maximum of χ'', which looks like a superimposition of several lines. To get a good fit for this part of the spectra, three lines

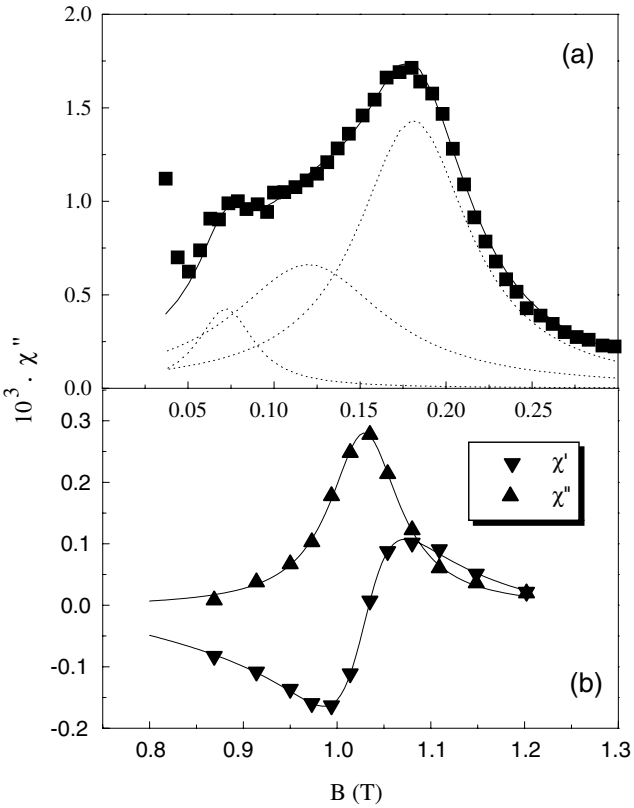

Figure 3. (a) Imaginary part of the magnetic susceptibility as a function of B_0, when B_0 is parallel to [110] and B_1 is parallel to $[1\bar{1}0]$. The temperature is $T = 30$ mK. The full line has been obtained by fitting the experimental data with the sum of three Lorentzian lines. These three curves have been plotted individually with dotted curves. (b) Real and imaginary parts of the magnetic susceptibility as a function of B_0, when B_0 is parallel to [110] and B_1 is parallel to $[1\bar{1}0]$. The temperature is $T = 40$ mK. The full lines have been obtained by fitting the experimental data with a Lorentzian line.

were needed. As the final agreement is very good (see figure 3(a)), it can be expected to be meaningful.

Line 6 has been plotted in figure 3(b), where it was the easiest one to fit, its shape being the usual one. The imaginary part of the susceptibility has been fitted with the standard formulae (2). For the real part, it was necessary to add a term proportional to $1/B_0$. Indeed, χ' decreases much more slowly than χ'', and there is a residual contribution of the former lines on the measured χ' around this resonance. At the first order, as the resonance field of line 6 is much higher than the other resonance fields, the residual contribution is proportional to $1/B_0$.

Finally, B_0 being still parallel to [110] but the oscillating field B_1 being parallel to [001], line 7 has been found. With B_0 parallel to [100], the line is still there, it has exactly the same shape, but it is shifted, it will be referred as line $7'$. Only line 7 has been plotted in figure 4. The shape is most unusual, as it is highly asymmetrical. It must be noted that $\sqrt{\chi'^2 + \chi''^2}$ would agree with a common Lorentzian behaviour. However, when looking at χ' and χ'', it does not hold. It was not possible either to fit χ' and χ'' with formulae (3) and (4), as was done for lines 1 and 2. Such a behaviour can be obtained if the splitting of the transition increases

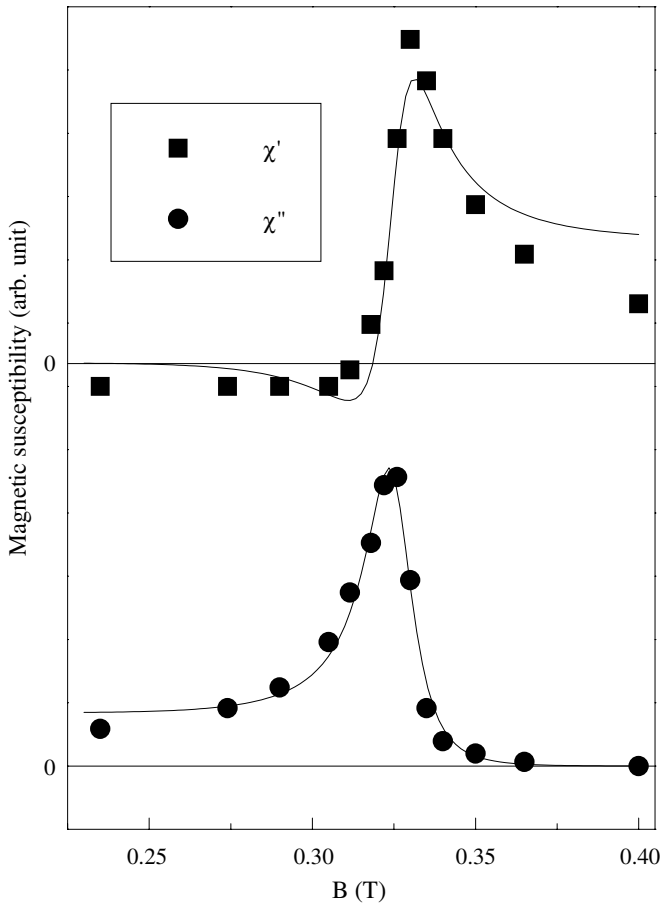

Figure 4. Real and imaginary parts of the magnetic susceptibility as a function of B_0, when B_0 is parallel to [110] and B_1 is parallel to [001]. The temperature is $T = 28$ mK. The straight lines are the results of fitting with theory. χ' and χ'' have been arbitrarily shifted, so that it is easier to compare them with the fits.

non-linearly with the magnetic field. Using the splitting ΔE instead of the magnetic field and the gyromagnetic ratio, χ' and χ'' can be written in the following way [28]:

$$\chi' = \frac{K(\Delta E/\hbar - \omega)T_2^2}{1 + (\Delta E/\hbar - \omega)^2 T_2^2}\chi_0$$
$$\chi'' = \frac{K T_2}{1 + (\Delta E/\hbar - \omega)^2 T_2^2}\chi_0 \tag{5}$$

where K is a constant, which includes the coupling factor and the density of spins. For rare-earth ions in uniaxial anisotropy, the following dependence for ΔE has been found [1]:

$$\Delta E = \sqrt{(g_J \mu_B J B_0 \cos\alpha)^2 + (\zeta (B_0 \sin\alpha)^{2J+1})^2} \tag{6}$$

where α is the angle between the anisotropy axis and the applied magnetic field and ζ is a constant depending on the anisotropy. The anisotropy is not the same here as in [1], but it has been shown that other anisotropies could give rise to the same behaviour [9] and, indeed, it has been possible to get a very good fit of the experimental data using equations (5) and (6).

The characteristics of all these lines have been summarized in table 1.

Table 1. Summary of the characteristics of the different resonance lines found in the crystal.

Line	B_0-direction	B_1-direction	Resonance field B_R (mT)	Linewidth (mT)	Shape of the line
1	[001]	[110]	41.1	6.8	Lorentzian
2	[110]	[1$\bar{1}$0]	6.8	4.5	Lorentzian
2′	[100]	Unknown	7.15	3.3	Lorentzian
3	[110]	[1$\bar{1}$0]	72	20	Lorentzian
4	[110]	[1$\bar{1}$0]	118	54	Lorentzian
5	[110]	[1$\bar{1}$0]	180	40	Lorentzian
6	[110]	[1$\bar{1}$0]	1029	42	Lorentzian
7	[110]	[001]	329	8.8	Anomalous
7′	[100]	[001]	275	9.2	Anomalous

5. Analysis

5.1. Orientation effect on the low field resonances

$LiYDyF_4$ is a well-known compound for laser applications and the spectroscopic properties of the Dy^{3+} ion in $LiYDyF_4$ have been determined through optical spectroscopy [29]. It has been shown that the lowest energy states were the 16 $^6H_{15/2}$ states. In zero field, as predicted by the Kramers theorem, each energy level is doubly degenerate. The energy of the first excited doublet is 14.2 cm^{-1} (20.42 K) above the ground doublet. At very low temperature and in a quite low magnetic field ($B_0 < 1$ T), only the lowest doublet can be expected to be populated. From this, an effective Hamiltonian with an effective spin $\tilde{J} = 1/2$ should be able to describe the spectra. As the frequency used is very low, hyperfine interactions may become important. In the case of dysprosium, there are essentially four possible isotopes, which are almost equally distributed in standard samples. Two of them have a non-zero nuclear spin (isotopes 161 and 163), where the nuclear spin I is equal to 5/2. From this, the Hamiltonian already successfully used in [21] can be expected to describe completely the energy spectrum (the normalized notations of [30] have been used here):

$$\tilde{H}_{eff} = g_{\parallel}\mu_B \tilde{J}_z B_z + g_{\perp}\mu_B(\tilde{J}_x B_x + \tilde{J}_y B_y) + A_{\parallel} I_z \tilde{J}_z + A_{\perp}(I_x \tilde{J}_x + I_y \tilde{J}_y) + P(I_z^2 - I(I+1)/3). \quad (7)$$

From isotopes 162 and 164, only one line is expected. Isotopes 161 and 163 are adding a hyperfine structure on the spectra. Assuming that only the most strongly allowed transitions are involved (transitions with $\Delta m = 0$), the hyperfine structure should exhibit six lines for each of these two isotopes. However, applying the relation $h\upsilon = |g_{eff}\mu_B B_R + Am|$ to get the resonance values (as a first step, the A values of [26] have been used), it can be shown that the lines are very close to each other: for B_0 parallel to [001], the 12 resonance fields range from 24 to 63 mT and for B_0 orthogonal [001], the 12 resonance fields range from 1 to 26 mT. In either case, using a very slow sweeping of the magnetic field, such a hyperfine structure could not be seen. It could be due to a lack of sensitivity of the apparatus as the intensity of these twelve lines are much lower than the main one due to isotopes 162 and 164. But, as the lines found seem to be quite wide, most probably the likely explanation is a large overlapping of the different hyperfine lines, making the fine structure disappear. Anyway, the purpose of this work was not hyperfine interactions and the main thing to remember about the first part of this analysis is the following: it seems that we do not have to care about hyperfine interactions.

The main result is the position of the lines: from them, the parameters $g_{\parallel}$ and $g_{\perp}$ can be calculated. $g_{\parallel}$ is found here equal to 1.18 instead of 1.11, as formerly found [20, 21]. This

difference is not meaningful, as a slight misalignment of 2.5° could explain it, and it can be concluded that agreement is good. It is becoming really interesting when looking at $g_\perp$: for B_0 parallel to [100], $g_\perp$ is found equal to 6.8, and for B_0 parallel to [110], $g_\perp$ is found equal to 7.15 instead of 9.2. First, there is a large difference with the previous results, which cannot be explained by some misalignment (35° would be needed, which can be excluded). It means that the splitting of the fundamental doublet does not rise linearly with the applied magnetic field. Implicitly, the use of an effective spin $1/2$ meant that first-order perturbation theory was suitable to describe the splitting. This non-linear behaviour suggests that this hypothesis was wrong and that the concept of effective spin $1/2$ cannot be used here. Such a behaviour could be due to a tunnelling effect arising from a fourth-order term of the type $(J_x^4 + J_y^4)$. Indeed, it has been shown [9, 16] that such a kind of term could give rise to a non-linear splitting. The second main result is a slight difference between the orientation [100] and [110]. Such a behaviour was predicted in [16], where a second-order difference was expected, which agrees quite well with the present experimental results. This is the first experimental evidence for such a phenomenon.

5.2. New resonance lines

From the previous analysis, it can be seen that the effective Hamiltonian (7) and hyperfine interactions cannot explain the other lines found. Indeed, from this Hamiltonian, no line was expected above 63 mT. Lines 3–5 could be due to pair effects, as the resonance field is around the dipolar interaction field between two next nearest Dy^{3+} ions. Indeed, for two next nearest neighbours, the dipolar field induced by one ion on the other one ranges from 190 to 380 mT, depending on the direction of the magnetic moment (the distance between two next nearest neighbours is 0.373 nm). To check this hypothesis, the best idea would be to study a more diluted sample, where the amplitude and the width of these lines should decrease quickly.

Lines 6 is more surprising: the resonance field is much too high for dipolar interactions to account for it and a pair effect can be rejected. It has been shown that hyperfine interactions could not explain an electronic resonance for this field, but a nuclear transition is possible. Indeed, roughly, the hyperfine contribution to the Hamiltonian is

$$H_{hyp} = A\vec{I} \cdot \vec{J}. \tag{8}$$

Using the A value of [26] and $15/2$ for J, this contribution of the Hamiltonian induces a splitting of 750 MHz for isotope 161, which is very near to the frequency used here. A small perturbation would be enough to bring it to around 680 MHz and make it possible to have a nuclear resonance with a magnetic field of 1 T.

Line 7 is maybe the most fascinating line. First, from its shape, it seems that the splitting of the fundamental doublet increases non-linearly with the magnetic field. The dependence of this splitting agrees with previous theoretical predictions for the tunnelling of large spins in a fourfold potential [9]. This is the first experiment which exhibits this kind of behaviour, and this is a very important result for spin-tunnelling theory. What is more, the coupling conditions are known. The oscillating field B_1 had to be parallel to the [001]: with B_1 in the easy plane the line could not be observed. This result is a very valuable test for future theories. Finally, a question must be posed: how can the value of the resonance field be explained? Indeed, the static field had the same direction as in the case of line 2, 3, 4, 5 or 6, but the resonance field seems to be quite different from all of them. The authors could not find any satisfactory answer to this question, which remains a fascinating enigma.

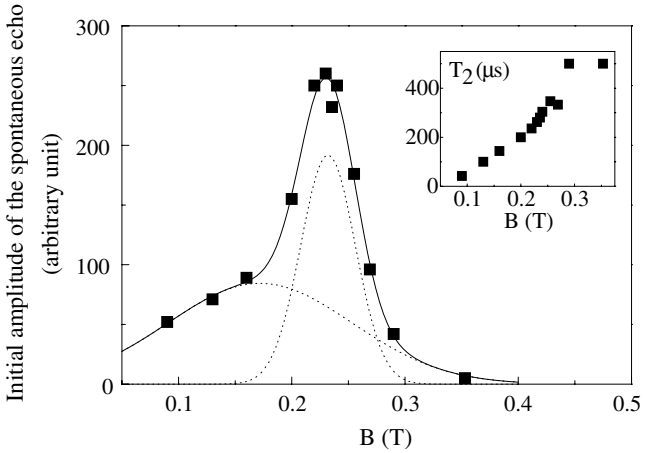

Figure 5. Initial extrapolated amplitude (i.e. amplitude when the delay between the two generating pulses goes to zero) of the spontaneous echo as a function of the magnetic field B_0. The static magnetic field B_0 is parallel to [100] and the oscillating magnetic field B_1 is parallel to [001]. The temperature is $T = 31$ mK. The duration of the pulses was 1.6 μs. The full line has been obtained by fitting the experimental data with the sum of two Gaussian lines. These two lines have been plotted individually with dotted lines. Inset: memory phase time T_2 as a function of the static magnetic field B_0. The magnetic static field B_0 was parallel to [100] and the oscillating magnetic field B_1 was parallel to [001]. The power was 1 dB corresponding to $B_1 = 1$ mT. The temperature was $T = 28$ mK.

6. Spin echoes

6.1. Amplitude of the spin echoes as a function of the magnetic field

It has been possible to observe spin echoes [25] in one particular configuration: B_0 was parallel to [110] and B_1 was parallel to [001]. To observe a spontaneous spin echo, the sample is subjected to two radiofrequency pulses, one beginning at $t = 0$, and one beginning at $t = t_{12}$. The duration of the pulses is assumed to be very short, compared to t_{12}. Then, at $t = 2t_{12}$, a spontaneous pulse, generated by the sample itself, can be detected in the cavity. This method is very sensitive, because the cavity is not excited by a radiofrequency pulse when the echo occurs and, as there is no parasitic power, very small signals can be extracted. The amplitude of the spontaneous echo depends on several parameters: the numbers of spins contributing to the echo, the amplitude of the rotating moments, the amplitude of the first two exciting pulses and the delay t_{12}. The amplitude decreases as a function of t_{12}. This decrease was well fitted by an exponential law and the characteristic decay time is the relaxation time T_2. Thus, it is possible to extrapolate the amplitude of the echo when t_{12} goes to zero. This extrapolated amplitude has been plotted in figure 5. It can be very well fitted with the superimposition of two Gaussian lines, as can be seen in figure 5. The first line is centred at 180 mT and the second one at 232 mT. The position of these two 'lines' is really surprising: with this configuration, only one line could be expected around 329 mT. Again, there is a fascinating enigma. Is there a connection between line 7 and these spin echoes? How is it possible to get large spin echoes around 232 mT, while nothing can be seen looking at χ' and χ''? The authors could not find any answers to these questions.

6.2. Phase memory

Spin echoes allow the determination of parameters difficult or impossible to get from classical EPR: the first one is the relaxation time T_2. If the line is not homogeneous, as seems to be the case here, the linewidth is due to the distribution of local magnetic field, not to T_2, and only spontaneous echoes can give access to T_2. T_2 as a function of B_0 has been plotted in the inset of figure 5. In the low range field, T_2 increases regularly with B_0, up to 0.3 T, where it seems to reach a plateau. As the line is highly inhomogeneous, it is not surprising to have a non-constant relaxation time. Qualitatively, the increase of T_2 with B_0 agrees with spectral diffusion theory [31, 32]. Spectral diffusion assumes that phase is lost because of the fluctuations of the precession pulsation, which arise from random spin flips. Indeed, when a spin flips near the observed ion, the internal magnetic field seen by the ion changes also. The phase memory time T_2 depends on the rate of the spin flips and on the density of spins which can flip. When B_0 increases, the fundamental state of the flipping spins changes. In low magnetic field B_0, the local fields are quite small, and thermal activation can easily flip many spins. A high rate for the spin flips can be expected. But, as B_0 increases, the energy spectra widen and many spins would not find the energy to flip in the thermal bath. The rate of the spin flips will go down and the phase memory T_2 should increase.

6.3. Determination of the coupling coefficient

The study of spin echoes gives access to a second parameter: the coupling coefficient γ_1. To get it, one must look at the amplitude of the spin echo as a function of the exciting pulses' area. The area, Θ, of a pulse is defined in the following way:

$$\Theta = \int \gamma_1 B_{1,0}(t)\,\mathrm{d}t \tag{9}$$

where $B_{1,0}(t)$ is the envelope of the high frequency pulse. It has been shown that the area $I(t_{12})$ of the echo depends quite simply on the area of the two generating pulses [32], t_{12} being the delay between the two generating pulses:

$$I = I_0 \cdot \sin\Theta_1 \cdot \sin^2(\Theta_2/2) \cdot \exp(-2t_{12}/T_2) \tag{10}$$

where I_0 is a constant and Θ_i is the area of the pulse i. Using two pulses of the same area, the experimental shape of the echo has been plotted in figure 6 for different values of the power. At low power (power lower than -15 dB), the echo has the shape of a single hump. The shape is the same as long as the power is lower than -15 dB. The effect of an increase of the power in this range is to increase the amplitude of the echo. Above -15 dB, a distortion appears: a negative hump grows on the beginning of the echo. As the power is increased, this negative hump increases and the positive hump reduces, until almost all the echo has become negative at -7 dB. If the power is increased again, the echo is no longer a single hump [28]: there are several oscillations (see -2 dB, (figure 6)).

The comparison with formula (10) is easy in the range of the low power, where there is a single hump and where the area is proportional to the amplitude. The amplitude of the echo has been plotted and fitted as a function of the power using formula (10). The result of the fit has been plotted with full curves in figure 7 for powers up to -13 dB and $B_0 = 0.230$ T. As can be seen, the agreement is very good. From this fitting procedure, the coefficient γ_1 is found equal to 0.5×10^9 s^{-1} T^{-1}. Above -13 dB, a qualitative comparison can be done: for $\Theta_1 = 3\pi/2$, all the echo should be negative. Using 0.5×10^9 s^{-1} T^{-1} for γ_1, $\Theta_1 = 3\pi/2$ corresponds to a power of -7 dB. This is in good agreement with the experimental result (figure 6). For powers above -7 dB, formula (10) is no longer sufficient to describe what is happening. From

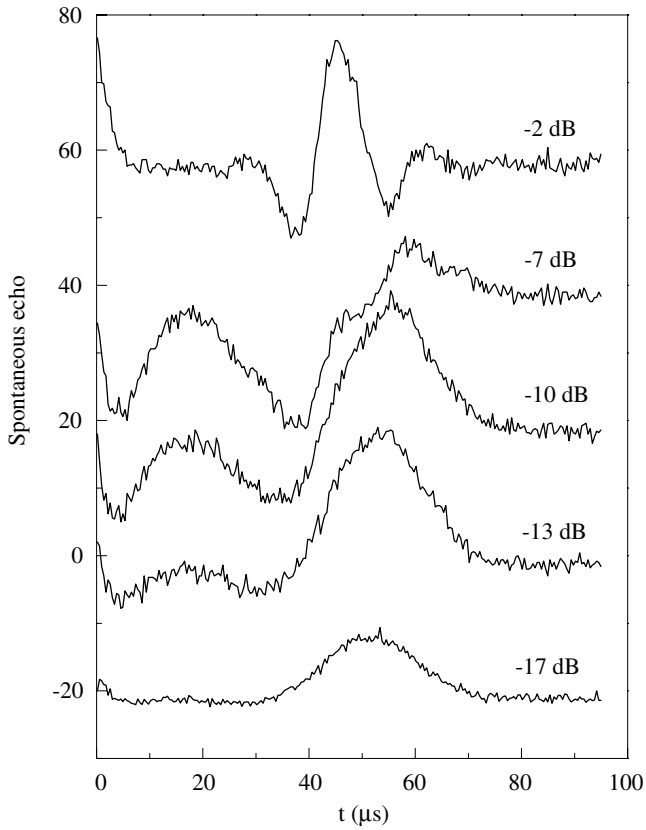

Figure 6. Shape of the spontaneous echo as a function of the power. The magnetic static field B_0 was parallel to [100] and the oscillating magnetic field B_1 was parallel to [001]. 0 dB corresponds to $B_1 = 1$ mT. The temperature was $T = 31$ mK, the duration of the first two pulses was 16 μs and the delay between these pulses was 70 μs. The echoes have been arbitrarily shifted, so that the shape can be better seen.

numerical simulations, assuming a wide distribution of internal magnetic field (inhomogeneous line) and the same coupling coefficient β for all the spins, several oscillations have been found for areas much bigger than π. So, the agreement is very good between the experimental results and what could be expected from theory.

This experiment has been done for three values of B_0 : 0.180, 0.230 and 0.266 T. The coupling coefficient has been found to be the same in these three cases. It must be said that no echo was found when B_1 was parallel to the easy magnetization plane, which could mean that γ_1 is much smaller in this configuration.

6.4. Fast relaxation in low magnetic field

Spin echoes were able to give very valuable information for B_0 in the range [90, 350 mT]. Unfortunately, no echo could be found below 60 mT, especially for the magnetic field around the resonance of lines 1, 2 and $2'$. This absence of echo can be attributed to two factors: the coupling coefficient γ_1 and the relaxation time T_2. If the coupling coefficient γ_1 is too small, the areas Θ_i are very small and, according to relation (10), the echo is too small to be detected.

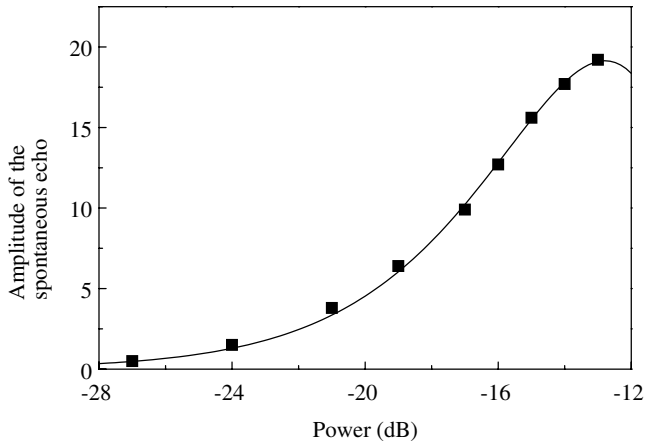

Figure 7. Initial amplitude of the spontaneous echo as a function of the power. The magnetic static field B_0 was parallel to [100] and the oscillating magnetic field B_1 was parallel to [001]. The temperature was $T = 28$ mK. 0 dB corresponds to $B_1 = 1$ mT.

However, as the standard χ-signal was big enough to be detected easily, this hypothesis does not seem to be the right one. The other possibility is a very short relaxation T_2. Indeed, the experimental set-up implied delays t_{12} between the two generating pulses greater than 10 μs. So, because of the decay according to $\exp(-t_{12}/T_2)$, spin echoes cannot be detected if T_2 is too short. In the present case, it would mean T_2 is shorter than 1 μs. This explanation does not contradict the existence of a high χ signal; contrary to γ_1, for an inhomogeneous line, the intrinsic relaxation time T_2 has no influence on the susceptibility, as can be seen from formula (3).

7. Conclusions

A set of experiments has been performed on a new interesting system for magnetic tunnelling: a crystal doped with Dy^{3+} ions, in which there is a fourfold symmetry. In this system, the magnetic moment of the Dy^{3+} ions are in an easy plane, with probably two easier axes, as is shown by the static susceptibility measurement presented here. Some of the features of this static susceptibility can be explained using the model of [16], which introduces a term of the type $(J_x^4 + J_y^4)$ in the Hamiltonian.

The low frequency electronic paramagnetic resonance spectra have been studied for three directions of the static magnetic field B_0: [001], [110] and [100]. Many resonance lines have been found. Three of them were predicted from experiments at higher frequency (10 GHz). However, for B_0 in the easy plane, the lines seem to be shifted compared to what was expected from the previous results at 10 GHz. What is more, the resonance field is slightly different for the [100] and [110] directions, contradicting existing knowledge. It has been shown that it could not be due to hyperfine interactions. Usually, as the first excited doublet is 20 K above the lowest one, only the latter is assumed to be involved, and the system is usually described by an effective spin $1/2$. This is probably where the description cannot account for what has been observed: an effect such as tunnelling involves all the states, and it is lost if one assumes the possible states to be in the space generated only by the two states of the fundamental doublet in zero field. Therefore the formalism of an effective spin $1/2$, which is a restriction to such a space, might induce an oversimplification of the spectra.

Several unexpected lines have also been found. Most of them cannot be explained by hyperfine interactions. They could arise from some pair effect, as the resonance field agrees with dipolar interactions between next neighbours. However, one of them has a resonance field much too high for such an explanation. It could be a nuclear resonance due to the very strong hyperfine interactions, which can induce a field very near the resonance value for the frequency used.

As some lines had very unusual shapes, an analysis of these shapes has been carried out. In the case of the low field lines, it was possible to explain the lineshape by the very low frequency of the spectrometer and the use of a linearly polarized oscillating field. An analytical formula to fit this lineshape has been found but it did not work for all the lines. For two of the lines, a non-linear dependence of the splitting as a function of the applied magnetic field had to be assumed. The non-linear law found agrees with the predictions for a tunnelling effect. This is a second piece of evidence for the occurrence of such an effect.

Spin echoes have been found. From this experiment, it has been possible to determine some coupling coefficients and relaxation time T_2. However, spin echoes could be found only in one configuration. Specifically, it was not possible to see spin echoes around the low field lines: the most probable explanation is a fast relaxation with T_2 shorter than 1 μs.

The system presented here seems to be a good experimental model for studying a magnetic moment in a fourfold potential. Some of the results obtained here were already predicted theoretically, but had never been observed experimentally. But there are also new data, with unexplained features. All these results should provide an interesting database to test the theories, which are beginning to arise in this field.

Acknowledgments

The authors wish to thank L Bouvot who made the resonator, J M Godard who prepared the sample, J Hammann who gave us access to the facilities of his SQUID magnetometer, C Faulkner and D Atkinson for their careful reading of the manuscript and S Ravy, F Beuneu, A Ginibre and P Mendels for instructive discussions.

References

[1] Korenblit I Ya and Shender E F 1978 *Sov. Phys.–JETP* **48** 937
[2] Chudnovsky E M and Gunther L 1988 *Phys. Rev. Lett.* **60** 661
[3] Van Hemmen J L and Sütö A 1986 *Europhys. Lett.* **1** 481
[4] Enz M and Schilling R 1986 *J. Phys. C: Solid State Phys.* **19** L711
[5] Garanin D A, Martinez Hidalgo X and Chudnovsky E M 1998 *Phys. Rev.* B **57** 13639
[6] Gunther L 1997 *Europhys. Lett.* **39** 1
[7] Prokof'ev N V and Stamp P C E 1998 *Phys. Rev. Lett.* **80** 5794
[8] Vernier N, Bellessa G and Parshin D 1995 *Phys. Rev. Lett.* **74** 3459
[9] Politi P, Rettori A, Hartmann-Boutron F and Villain J 1995 *Phys. Rev. Lett.* **75** 537
[10] Vernier N and Bellessa G 1993 *Phys. Rev. Lett.* **71** 4063
[11] Thomas L, Lionti F, Ballou R, Gatteschi D, Sessoli R and Barbara B 1996 *Nature* **383** 145
[12] Friedman J R, Sarachik M P, Tejada J and Ziolo R 1996 *Phys. Rev. Lett.* **76** 3830
[13] Wernsdorfer W and Sessoli R 1999 *Science* **284** 133
[14] Bellessa G, Vernier N, Barbara B and Gatteschi D 1999 *Phys. Rev. Lett.* **83** 416
[15] Del Barco E, Vernier N, Hernandez J M, Tejada J, Chudnovsky E, Molins E and Bellessa G 1999 *Europhys. Lett.* **47** 722
[16] Kalatsky V A, Müller-Hartmann E, Pokrovsky V L and Uhrig G S 1998 *Phys. Rev. Lett.* **80** 1304
[17] Kalatsky V A and Pokrovsky V L 1998 *Europhys. Lett.* **44** 539
[18] Vernier N and Bellessa G 1998 *J. Magn. Magn. Mater.* **177–181** 962
[19] Reich D H, Ellman B, Yang J, Rosenbaum T F, Aeppli G and Belanger D P 1990 *Phys. Rev.* B **42** 4631
[20] Mennenga G, de Jongh L J, Huiskamp W J and Laursen I 1984 *J. Magn. Magn. Mater.* **44** 48

[21] Sattler J P and Nemarich J 1971 *Phys. Rev.* B **4** 1
[22] Hardy W N and Whitehead L A 1981 *Rev. Sci. Instrum.* **52** 213
[23] Gurevitch A G 1963 *Ferrites at Microwave Frequencies* (New York: Consultants Bureau) p 247 (formulas (31.27) and (31.28))
[24] Lerbet F and Bellessa G 1986 *Cryogenics* **26** 694
[25] Hahn E L 1950 *Phys. Rev.* **80** 580
[26] Abragam A and Bleaney B 1986 *Electron Paramagnetic Resonance of Transition Ions* (New York: Dover)
[27] Zwillinger D (ed) 1996 *Standard Mathematical Tables and Formulae* (Boca Raton, FL: Chemical Rubber Company Press)
[28] Allen L C and Eberly J H 1975 *Optical Resonance and Two-Level Atoms* (New York: Wiley–Interscience)
[29] Gschneider Jr K A (ed) 1982 *Handbook on the Physics and Chemistry of Rare Earths* (Amsterdam: North-Holland)
[30] Rudowicz C and Sung H W F 2001 *Physica* B **300** 1
[31] Klauder J R and Anderson P W 1962 *Phys. Rev.* **125** 912
Mims W B 1968 *Phys. Rev.* **168** 370
[32] Mims W B 1972 *Electron Paramagnetic Resonance* ed S Geschwind (New York: Plenum) pp 263–351